Article

Stability Analysis and Network Topology Optimization of Multi-Agent Systems for Material Transport in Industrial Parks

Jichao Fei [1], Linfeng Zhang [2], Xiaorong Zhu [1,*] and Yiming Wu [1]

1   College of Telecommunications and Information Engineering, Nanjing University of Posts and Telecommunications, Nanjing 210003, China
2   China Telecom Corporation Limited Research Institute, Guangzhou 510630, China
*   Correspondence: xrzhu@njupt.edu.cn

Abstract: Multiple Automated Guided Vehicles promise to be an effective solution for executing tasks such as material transportation and inspection in industrial parks. In particular, system stability is the key to maintaining connectivity among multiple agents. In this paper, we build the stability model of multi-agent system (MAS) under the background of swarm robots transporting materials in an industrial park, and propose a network topology optimization method to improve the stability of MAS. In concrete, we first analyze the effect of channel environment on network topology, and the communication delay is analyzed. Then considering the communication delay and artificial potential field, we establish the stability analysis model of MAS and obtain the stability condition of the MAS by using Lyapunov correlation theorem. Finally, we formulate the network topology optimization problem of MAS by maximizing the second smallest eigenvalue of the Laplacian and get the optimal solutions. Analysis and simulation results show the effectiveness of the proposed model and algorithm.

Keywords: industrial parks; MAS; system stability; network topology

1. Introduction

The industrial Internet is an important driving force for the intelligent transformation of the global industrial system and an important cornerstone for the deployment and implementation of intelligent manufacturing. In recent years, multi-agent system (MAS) has attracted extensive attention. With the continuous development of multi-agent technology, multi-agent system has been particularly applied in military, industrial and other fields. In industry, logistics play a crucial role in economic growth. However, the logistics industry is still facing the problem of high cost and low efficiency. The development of intelligent logistics brings opportunities to solve these problems. The traditional warehousing and logistics system use a lot of manpower to carry, load and unload materials. This results in low overall work efficiency and poor consistency. Industrial Internet integrates industrial system, Internet, sensing technology and edge computing to reconstruct the industrial system and improve the working efficiency of industrial parks. In the 5G industrial Internet scenario, Automated guided vehicle (AGV) plays an increasingly important role in logistics. AGV can reduce the complications that come with manual handling and improve the efficiency of material transportation in the entire industrial park. When a single AGV executes a task, the execution efficiency of the task is affected due to the constraints of its own hardware conditions. If the task assignment information is sent to each AGV, resources are also wasted. Therefore, multi-agent formation should be introduced to complete the task cooperatively.

In the industrial park system based on swarm robots, AGVs are divided into clusters. A cluster of AGVs completes a set of customer orders together, and each order contains several items. In multi-AGV transportation, tasks should first be assigned to the leader of

each cluster, and then the AGVs of each cluster should guarantee the completion of the task without collision and stably. In this process, because clusters need to be uninstalled cooperatively, this paper also considers the information interaction between multiple clusters. When other clusters have information (such as computing resources and decision information) needed by the current cluster for edge computing, connections are established between clusters and information is transmitted, which facilitates the calculation and uninstallation planning and other tasks.

The core idea of MAS is to divide and conquer. We hope to decompose a complex dynamic system into relatively independent subsystems and accomplish complex tasks through the cooperation between subsystems. MAS needs to realize the organic linkage of different production links, and each agent has different resources and design technical indexes. In addition, the cooperation of multiple agents needs to ensure the connectivity of the intra-cluster AD hoc network. Stability is also an important factor to maintain the connectivity between agents in a cluster. Therefore, the research of multi-agent mainly focuses on the cooperation between multi-agents and the stability of the whole network. In addition, considering the complexity of the industrial environment, obstacle avoidance is also essential for AGVs to complete tasks [1]. This paper studies the stability of MAS under the background of swarm robots transporting materials in an industrial park, and proposes a stability analysis model and a topology optimization method to improve the stability of MAS. In concrete, the contributions of this paper are as follows:

- We establish a network topology analysis model for the stability of MAS, which considers the characteristics of wireless communication, including channel fading, antenna transmit power and networking mode. Based on these factors, the adjacency matrix representing the inter-AGVs network and the connectivity between the leader and the base station is defined. In addition, the communication delay in the whole control process is considered more comprehensively. We design the control flow, and verify the influence of the channel environment on network topology and system performance.
- The stability analysis model of the multi-agent cooperative system is established. Based on the background of material transport and processing in industrial parks with swarm robots, AGV groups with the same task are defined as a cluster, and information interaction between clusters is carried out through MEC. While controlling the relative distance of AGVs in the cluster, we also introduce artificial potential field function to plan the potential field relationship between each node, and obtain the dynamic equation of AGVs. Thus, we can obtain the stability analysis model within the cluster. Then the stability conditions are derived by the Lyapunov correlation theorem and verified by simulation.
- Finally, since the second smallest eigenvalue of the Laplacian matrix of the formation topology adjacency matrix is an important index affecting the control stability of the system, the topology optimization is carried out by maximizing the second smallest eigenvalue of the Laplacian operator. Then, the optimal topology including AGVs and MEC in the industrial Internet environment is obtained by combining the scenario and channel environment.

2. Related Works

Nowadays, with the booming development of industrial Internet and MAS, there are many researches on cooperative control of MAS [1–12]. In [2], the consistency of second-order heterogeneous MAS is investigated, and the consistency of position information and velocity information is comprehensively considered. The heterogeneous system is composed of linear and nonlinear second-order agents, among which the nonlinear agents have different structures. In addition, the coupling phenomenon exists widely in the real world. For example, the coupling phenomenon of nodes in complex networks is introduced in [3], and the coupling function among nodes in these networks is usually nonlinear. The coupling phenomenon also exists in MAS, which makes the system more consistent

with the real world. The delay in MAS is mainly divided into communication delay [3] and input delay [4]. The communication delay is related to the information exchange among agents, and the input delay is mainly related to the performance of agents in processing information. The main analysis methods of multi-agent time-delay systems are the frequency domain method and the Lyapunov function method [4]. Above researches do not consider adaptive coupled MAS. In practice, MAS with internal coupling and external adaptive coupling is more practical. There are also some studies considering adaptive topology. Finite-time and fixed-time protocols are proposed in [5] to solve the consensus problem in multi-agent systems with time-varying directed topologies. In [6], time-varying formation control of fractional-order MASs with general linear dynamics is studied under fixed and switched directed interaction topologies. A distributed control protocol based on observer is proposed to realize time varying formation control.

Multi-agent group cooperative motion control first assumes the motion model of each agent in the group, and then designs the corresponding control strategy according to the individual motion model. In a control strategy, the behavior of each agent needs to react according to its neighbors. Although the actual movement state of each agent is not preset, the collective intelligent behavior of cooperative movement will emerge. In addition, if the agent encounters obstacles or other agents that do not belong to the same subsystem in the process of movement, the original control strategy cannot meet the stability requirements of the system, which requires the introduction of a control model with an obstacle avoidance function. It is pointed out in [1] that a group is composed of an indefinite number of individuals, and the relative motion among individuals in the group and the macro motion of the whole group in the external environment are derived from the attractive and repulsive forces in the existing "potential field". The potential field can be a real physical repulsive or attractive force, or it can be an artificial potential energy function set by mathematics. Different choices of artificial potential energy function can reflect the diversity of clustering behavior.

The obstacle avoidance function of MAS based on artificial potential field is also a hot topic [7–9]. In [7], two main spatial constraints are defined mathematically: boundary and barrier, and unifies them into a general expression of artificial potential function. In [8], a formation control method of virtual leader integrated with the artificial potential field was adopted, and a distributed second-order consistency control method based on virtual leader was adopted to realize the formation function of multi-UAV system according to a certain formation, and the function of all UAVs in the system tracking the virtual navigator in formation. In [9], the efficient perception and obstacle avoidance of multi-UAV systems in the context of aerospace industry has been studied. However, the influence of delay on MAS control is not considered in the above papers. In terms of delay, the influence of network delay is considered in [10] and a network-based leader-follower consensus protocol with a heterogeneous gain matrix for each follower agent is proposed. However, obstacles are not considered in this paper.

At present, there are few research works on the optimization of MAS communication topologies using control theory. In [11], Hao explores the influence of channel fading on control from the perspective of communication, and analyzes the classical control theory used in traditional formation from the perspective of communication topologies. In addition, a unified optimization framework is proposed in [12]. At the same time, the weight of the primary communication graph edge is reduced to optimize the network topology and ensure the consistency and adjustable convergence rate of the uncertain multi-agent system. However, these papers did not consider the influence of delay on control.

It is seen from the existing research works that although the formation control and obstacle avoidance control are classical control, the two aspects of research in the field of control has been gradually mature, but for multi-agent, especially the AGV fleet communication topology is less. Seldom research considers formation and obstacle avoidance of refining time delay that exist in the system at the same time. The influence of topology on system stability is also not considered. Aiming at the above problems, we study the stability

of MAS under the background of swarm robots transporting materials in an industrial park, and proposes a stability analysis model and a topology optimization method to improve the stability of MAS.

3. System Models

In this paper, we consider the scenario of multiple AGVs cooperatively delivering tasks in the industrial Internet, as shown in Figure 1, which is divided into the device layer, the edge layer and the cloud layer. In the device layer, it is assumed that AGVs are divided into several clusters to complete the material delivery task cooperatively. Each cluster has a cluster head, and the cluster head can carry out information interaction between the two clusters to complete resource allocation cooperatively. The AGVs in the cluster interact with each other to make a formation. The leader moves towards the target point and then pulls other AGVs to move.

The edge layer consists of several edge nodes, each of which includes 5G base station, MEC, etc. Each edge node manages a portion of the region. Each edge node is only responsible for the management of obstacle information and real-time control of agv in its own area. The control commands issued by the edge nodes enable AGVs to avoid obstacles in real-time.

The cloud layer is responsible for providing the operation interface for operators, sending tasks and instructions to edge nodes, and then assigning tasks to all leaders. According to the tasks given by the cloud service layer, the AGVs carry out automatic identification and transfer, and pull leaders by setting target points. After reaching the target point, the operator completes the material registration and picks up the material. Then, according to the instructions of the cloud layer, the AGVs choose to continue the delivery or wait in the designated area.
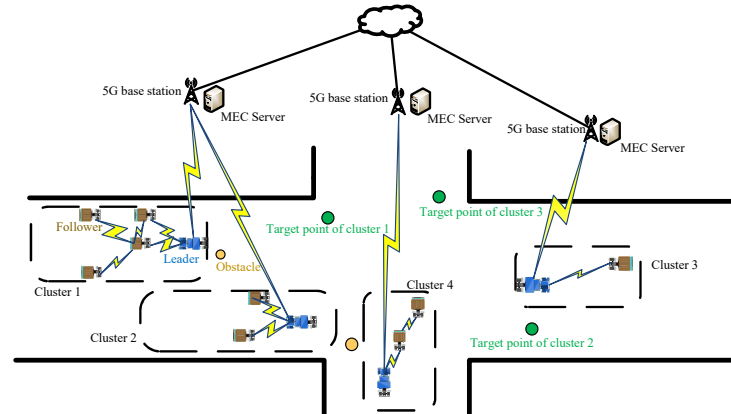
Figure 1. The structure of the industrial park. The scenario is divided into three layers: the cloud layer, the edge layer, and the device layer. The cloud layer is mainly responsible for assigning tasks and setting target points. The AGVs in the device layer are connected adaptively by Wi-Fi. They are grouped and travel to the target point to complete the transport task, during which they need to avoid obstacles. The leader of each cluster is connected to the edge layer device using 5G.

In this paper, Wi-Fi Mesh network is assumed to be used for communication between AGVs in the cluster. Leaders are connected to servers in the edge layer through 5G. Before each cluster starts executing tasks, the leader is selected in the cloud layer. The AGV with the best performance such as integrated communication computing capacity and battery capacity is selected as the leader. The voting and leader selection is one of the core parts in MASs, but this is not the focus of this paper. Therefore, we only describe it briefly. The leader uses his own camera to determine the location of obstacles in his surroundings. AGVs with better communication quality (that is, the communication signal-to-noise ratio is greater than a certain threshold) among all the AGVs within the communication range are selected to establish connections. If the SNR between the two AGVs is too low

due to various reasons during the movement, the connection will be disconnected. If the probability of SNR greater than a certain value in the driving process of two AGVs without communication is higher than a certain threshold, a connection will be established between the two AGVs. Compared with the centralized communication architecture, this communication mode reduces the excessive requirements on the communication ability of leaders, and makes the communication topology not fixed but adjustable. In addition, all AGVs need to sense the surrounding environment, keep a safe distance from other AGVs and obstacles, and keep a safe distance from other communicating AGVs. Therefore, it is necessary to preset the ideal distance between each AGV and the leader and set the artificial potential field function. In this scenario, formation control and obstacle avoidance control are considered for the stability of the system.

3.1. Connectivity Topology Model of Multi-AGV Communication Network

The primary problem of cluster control for agents in industrial parks is to establish a proper communication network for interactive transmission of information in MASs. In this paper, we consider clustering all AGVs in the workshop according to task requirements, and AGVs in each cluster can establish self-organizing communication networks to achieve efficient data transmission and information interaction.

In the scenario envisaged in this paper, the AGV in an industrial park is divided into several clusters according to task requirements, and we first consider cluster i. Assuming that there are N agents in the cluster. The AGV with the strongest ability is selected as the leader and denoted as the Nth agent by comprehensive communication and computing capability and battery capacity. Their weighted graph is denoted by $W = \{V, E, A\}$, where V represents the AGVs node, E represents the edge between adjacent AGVs, and A represents the adjacency matrix composed of AGVs in the cluster. The Laplace matrix is denoted by $\Delta = De - A$, De is the degree matrix. Considering that in practice, nodes need to frequently exchange position information and control signals, data transmission needs to meet the requirements of reliable data transmission, and the adjacency matrix is improved to the communication quality matrix [11]. Where, elements represent the connectivity between two nodes, that is, the probability of successful communication, so as to reflect the characteristics of the channel environment where the two nodes reside: $a_{ij} = p_\gamma^{ij}(\Gamma_{ij}(t) > \gamma) = e^{-(\sigma^2 \gamma (d_{ij})^n)/(G_{ij}^a P_{ij})}$. Where d_{ij} represents the distance between two AGVs, The average power of the noise in the wireless channel is σ^2, and the AGVs carries a directed antenna with gain G_{ij}^a, so that the nodes have different gains in the direction of other nodes. There are controllable transmit power P_{ij} in different directions. n represents the path loss index, which increases with the increase of obstacles. The value ranges from 2 to 6. If it is 2, it represents the free space environment. When the gain of the fading channel is $G_{ij}(t)$, the SNR between node j and node i can be expressed as: $\Gamma_{ij}(t) = \frac{P_{ij} G_{ij}(t)}{\sigma^2}$, where $G_{ij}(t) = \frac{G_{ij}^a |h_{ij}|^n}{(d_{ij})^n}$. Sufficient SNR is required for data transmission. Assuming that the probability of SNR greater than γ is greater than a certain threshold p_{th}, two agents can communicate successfully. h_{ij} is a Gaussian process with zero mean and unit variance. Thus can calculate the agent i and the probability of successful communication is between agent j: $p_\gamma^{ij}(\Gamma_{ij}(t) > \gamma) = exp(-\frac{\sigma^2 \gamma (d_{ij})^n}{G_{ij}^a P_{ij}})$. Then $a_{ij}(t) = 1$ if $p_\gamma^{ij}(\Gamma_{ij}(t) > \gamma) \geq p_{th}$. Otherwise, $a_{ij}(t) = 0$. If the value is greater than a certain threshold, agent i and agent j are connected, which represents the topological switch. In addition, this paper adopts two-way communication, that is, $a_{ij}(t) = a_{ji}(t)$.

Since the leader needs to collect the location information of obstacles and transmit this information to the MEC of the edge layer for calculation to generate control instructions and then send them to AGVs, the uplink rate of data transmission of the leader needs to be considered. We use Shannon's formula [13] to calculate the channel capacity between the leader of the ith cluster and the kth base station: $Ca_{ik} = W_k log_2(1 + \frac{P_i G_i^a d_{ik}^{-n}}{n_0 W_k})$, where W_k represents the kth the bandwidth of the base station, P_i represents the transmitted power of

the leader of the *ith* cluster, G_i^a represents the antenna gain of the leader of the *ith* cluster, and d_{ik} represents the distance from the leader of the *ith* cluster to the *kth* base station. By calculating the transmission rate between the leader and the base station, we can determine which base station to connect with through 5G. In this paper, we choose to connect to the base stations with higher average transmission rates over a short period of time. In the network-based control scenario, the transmission between agents occurs only at each sampling time, that is, only at time t_k, and then the topology remains unchanged until the next sampling starts.

3.2. Delay Analysis of MAS within a Cluster

In this paper, the controller inside the leader of each cluster is considered as the controller of all AGVs in this cluster. Different from the scenario in [10], we consider that the AGV transmits signal to the MEC, and then the MEC transmits the control signal to the controller in the leader. Finally, the leader transmits the signal to the actuator of each AGV. The control process structure of the multi-AGVs cooperative system is shown in Figure 2. Each agent operates remotely through the communication network, resulting in network delay in information transmission, including:

- The AGV sends information to neighboring nodes through the sampler, and then to the MEC through the leader. After receiving the data packet, the neighbor nodes also transmit their location information from their own samplers to the leader through Wi-Fi, and then transmits it to the MEC through 5G for calculation. So, it is necessary to queue, MEC again after the calculation and then send the control signals to the leader. There is a queuing delay in MEC during this process.
- The latency in the process of MEC transmitting the calculated control signals to the leader controller through 5G network.
- The leader's controller also needs to transmit the control signals to the internal actuators of AGVs through Wi-Fi, and this process also contains time delay.
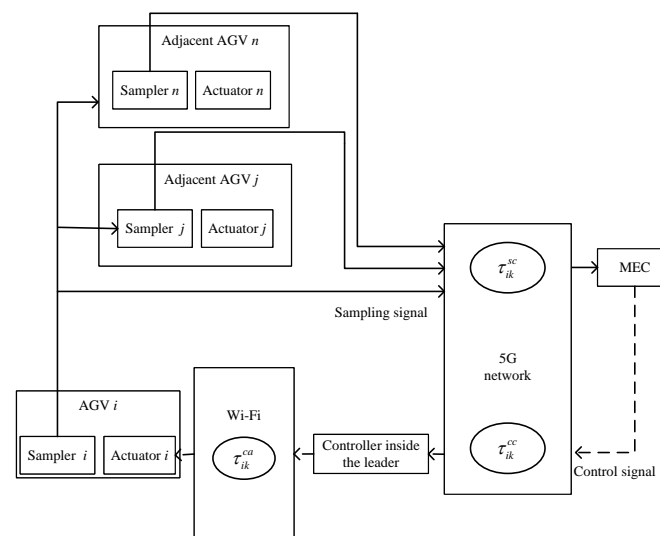
Figure 2. Control process structure of multi-AGV cooperative system. The time delay of signal transmission is analyzed. The ellipse represents the time delay that occurs during the process. Solid arrows represent sampling signals and dotted arrows represent control signals.

In this paper, it is assumed that no packet loss or disorder occurs. The information of each agent *i* is sampled by the sampler in AGV in a period of *h*, and the sampled data can be sent to other AGVs by Wi-Fi, and to MEC by 5G through the leader, and then the information is sent to the controller of the leader after MEC calculation. Finally, the controller of the leader sends the control signals to the actuator in agent *i*. The *k*th sampling time is denoted as t_k, then $0 < t_{k+1} - t_k = h_k \leq h$. Due to the influence of time delay,

the sampled data from agent i and neighboring agent j will arrive at the MEC of the edge layer at different times, and all the data are queued in the MEC. Therefore, MEC also plays the role of storing the received location information until all the information transmission of agent i is completed, and then the location information will be calculated. From the MEC, the calculated control signals is sent to the leader's controller. Finally, the controller of the leader sends the control signals to agent i, and the actuator in agent i completes the movement process. In this process, there is also a delay of information transmission between the MEC and the controller of the leader and the controller of the leader and the agent i.

τ_{ij}^{sc} on behalf of the agent i and its adjacent agent j sampler to transmit data calculation and the communication time delay to the MEC, The delay of agent i at this stage is defined as $\tau_{ik}^{sc} = max_i\{\tau_{ij,k}^{sc}|j \in i \cup N_i\}$, N_i represents the adjacent AGV collection of i. τ_{ik}^{cc} is the communication delay from the MEC of the edge layer to the controller of the leader. τ_{ik}^{ca} is the communication delay from the controller in the leader to the actuator of agent i. So the total delay is $\tau_{ik} = \tau_{ik}^{sc} + \tau_{ik}^{cc} + \tau_{ik}^{ca}, i = 1, \ldots, N$. Define all AGVs in the distributed MAS in the kth sampling time control process of total delay as $\tau_k = max_i\{\tau_{ik}|i = 1, \ldots, N\}$, we assume that τ_k is also bounded, $\tau_m \leq \tau_k \leq \tau_M$.

4. Stability Analysis of MAS

4.1. Stability Aalysis of MAS within a Cluster

4.1.1. Design of Governing Equations

We refer to the three basic rules proposed by Reynolds [14] for the group behavior of agents: (1) Separation: the agent and its neighboring agents avoid collision; (2) Aggregation: the agent should be compact with its neighboring agents, and the distance should not be so large that the cluster is disconnected and divided into two clusters; (3) Consistency: the agent should keep consistency with its neighboring agents. On this basis, the attractive force of the target point is also added. The motion of each agent is affected by the position of all the agents in its neighborhood.

Consider a set of MASs consisting of N AGVs, where the dynamic equation of each AGV is as follows:

$$\dot{x}_i(t) = Bx_i(t) + u_i(t) \tag{1}$$

where, $x_i(t)$ represents the position of agent i, $B \in \mathbb{R}^{N \times N}$ is a constant matrix, $u_i(t)$ represents the governing equation of the external input.

AGVs will actively control the position of its neighboring AGVs:

$$e_i^x(t) = \sum_{j=1}^{N} a_{ij}(t_k)\left(x_i(t_k) - x_j(t_k) + r_i - r_j\right) \tag{2}$$

where $t_k + \tau_k \leq t \leq t_{k+1} + \tau_{k+1}$, r_i represents the ideal distance between agent i and leader to form the desired formation.

In summary, the formation control considering delay and time-varying topology is given by:

$$u_i^f(t) = -Ke_i^x(t) \tag{3}$$

where K represents the feedback gain matrix, $K \in \mathbb{R}^{N \times N}$

As described at the beginning of this section, each AGV can obtain the location information of surrounding obstacles (including agents of other clusters and external obstacles) through edge nodes. In this paper, AGVs are regarded as particles, the communication radius is r, the distance between AGVs in the cluster is not less than d_α, and the expectation between AGVs and obstacles is d_β. The force of AGVs is the combined force composed of the forces of other AGVs and the repulsive force of obstacles, while the leader is also attracted by the target point.

As shown in Figure 3, taking the leader as the reference point, the target point will generate an attractive force on the leader, so that it can move to the target point to complete the transportation task. Secondly, if the distance between the follower and the leader is too small, a repulsive force will be generated between the leader and the follower. Finally, the distance between obstacle 1 and the leader is not less than the ideal distance d_β, so no extra force is applied. However, the distance between obstacle 2 and the leader is too small, so the obstacle needs to exert a repulsive force on the leader. The whole process is also affected by the ideal distance between all AGVs and the leader set before.
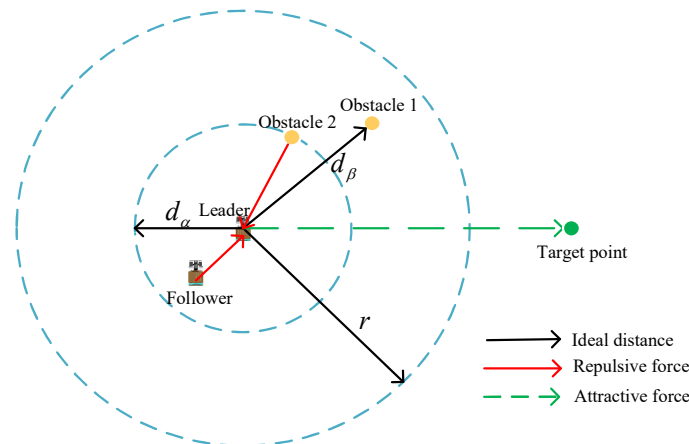
Figure 3. Schematic diagram of the potential field of the leader. Followers will not be attracted by the target point. d_α Indicates the minimum distance between AGVs. d_β Indicates the minimum distance between an AGV and an obstacle. r is the maximum communication radius of the AGV.

We first consider the gravitational force at the target point. The attractive force is proportional to the distance between them. Denote the target point as x_{tar}.

$$u_i^{ta}(t) = -\nabla \Psi_t(\|x_i(t_k) - x_{tar}\|)d_i \tag{4}$$

where, d_i is equal to 1 only when $i = N$, and equal to 0 in other cases, indicating that the target point only exerts force on the leader, and then the leader pulls other AGVs to move. The function $\Psi_t(\|x_i(t_k) - x_{tar}\|)$ needs to be satisfied so that the potential field force is proportional to the distance between leader and the target point. It is also necessary to control the force not to be too large, otherwise it will affect the maintenance of the formation.

So in this paper, the following function is used:

$$\Psi_{ta}(\|x_N(t_k) - x_{tar}\|) = \begin{cases} \frac{1}{2}\mu_1 \|x_N(t_k) - r\|^2 & \|x_N(t_k) - x_{tar}\| > r \\ \frac{1}{2}\mu_1 \|x_N(t_k) - x_{tar}\|^2 & \|x_N(t_k) - x_{tar}\| \leq r \end{cases} \tag{5}$$

where μ_1 denotes the attractive force field constant. The negative gradient of the above function is obtained, and the expression of the attractive force of the target point to the leader is:

$$u_i^{ta}(t) = d_i u_i^{ta}(t_k) = \begin{cases} -d_i\mu_1 \|x_N(t_k) - r\| & \|x_i(t_k) - x_{tar}\| > r \\ -d_i\mu_1 \|x_N(t_k) - x_{tar}\| & \|x_i(t_k) - x_{tar}\| \leq r \end{cases} \tag{6}$$

where $t_k + \tau_k \leq t \leq t_{k+1} + \tau_{k+1}$.

Consider the separation and the aggregation criteria, starting with the internal obstacle avoidance. If there is information interaction between agent i and agent j, let $\|x_{ij}\| = \|x_j - x_i\|$, for agent i, the internal potential field between agent i and all other AGVs is:

$$\Psi_i = -\sum_{j \in N_i} \Psi_{ij}(\|x_{ij}\|) \tag{7}$$

If $\|x_{ij}\| < d_\alpha$, then there is a repulsive force field. In this paper, the function $\Psi_{ij}(\|x_{ij}\|)$ is defined as follows:

$$\Psi_{ij}(\|x_{ij}\|) = \frac{1}{2}\mu_2\left(\frac{\|x_{ij}\|}{d_\alpha} + \frac{d_\alpha}{\|x_{ij}\|} - 2\right) \tag{8}$$

The negative gradient of the above equation is obtained, and the potential field forces of agent i and agent j are expressed as:

$$u_{ij}^\alpha(\|x_{ij}(t_k)\|) = \begin{cases} -\frac{1}{2}\mu_2\left(\frac{1}{d_\alpha} - \frac{d_\alpha}{\|x_{ij}(t_k)\|^2}\right) & \|x_{ij}(t_k)\| \leq d_\alpha \\ 0 & \|x_{ij}(t_k)\| > d_\alpha \end{cases} \tag{9}$$

where μ_2 denotes a constant, $t_k + \tau_k \leq t \leq t_{k+1} + \tau_{k+1}$.

The inter-AGVs obstacle avoidance control input within the cluster is finally defined as:

$$u_i^\alpha(t) = \sum_{j \in N_i} u_{ij}^a(\|x_{ij}(t_k)\|) \tag{10}$$

Finally, external obstacle avoidance is considered, that is, obstacle avoidance control between AGVs and obstacles. For the convenience of calculation, all obstacles are set as particles, $ob = \{o_1, o_2, \dots, o_n\}$ is the set of obstacle positions. If the distance between AGVs and obstacles is greater than or equal to d_β, then the repulsive force is 0. If the distance is less than d_β, the repulsive force exists. To meet the described scenario, set the function as follows:

$$\Psi_\beta(\|x_i(t_k) - o_h(t_k)\|) = \begin{cases} \psi_\beta & \|x_i(t_k) - o_h(t_k)\| \in (0, d_\beta) \\ 0 & \|x_i(t_k) - o_h(t_k)\| \in [d_\beta, \infty) \end{cases} \tag{11}$$

where $\psi_\beta = \mu_3\left(\frac{1}{\|x_i(t_k)-o_h(t_k)\|} + \frac{\|x_i(t_k)-o_h(t_k)\|}{d_\beta^2} - \frac{2}{d_\beta}\right)$.

The negative gradient of the above equation is obtained as follows:

$$u_{ih}^\beta(\|x_i(t_k) - o_h(t_k)\|) = \begin{cases} -\dot{\psi}_\beta & \|x_i(t_k) - o_h(t_k)\| \in (0, d_\beta) \\ 0 & \|x_i(t_k) - o_h(t_k)\| \in [d_\beta, \infty) \end{cases} \tag{12}$$

where $-\dot{\psi}_\beta = \mu_3\left(\frac{1}{\|x_i(t_k)-o_h(t_k)\|^2} - \frac{1}{d_\beta^2}\right)$, μ_3 denotes a constant and $t_k + \tau_k \leq t \leq t_{k+1} + \tau_{k+1}$.

So the control equation for the external obstacle avoidance of the agent i is:

$$u_i^\beta(t) = \sum_{j \in N_{io}} u_{ih}^\beta(\|x_i(t_k) - o_h(t_k)\|) \tag{13}$$

where N_{io} represents the set of obstacles that will exert force on agent i.

In summary, the overall governing equation is:

$$\begin{aligned} u_i(t) &= u_i^f(t) + u_i^t(t) + u_i^a(t) + u_i^\beta(t) \\ &= -K\left[\sum_{j=1}^N a_{ij}(t_k)(x_i(t_k) - x_j(t_k) + r_i - r_j)\right] \\ &\quad + d_i u_i^{ta}(t_k) + \sum_{j \in N_i} u_{ij}^a(\|x_{ij}(t_k)\|) \\ &\quad + \sum_{j \in N_{io}} u_{ih}^\beta(\|x_i(t_k) - o_h(t_k)\|) \end{aligned} \tag{14}$$

where $t_k + \tau_k \leq t \leq t_{k+1} + \tau_{k+1}$. Then the equation of state of AGV i can be expressed as:

$$
\begin{aligned}
\dot{x}_i(t) = {} & Bx_i(t) - K\left[\sum_{j=1}^{N} a_{ij}(t_k)\big(x_i(t_k) - x_j(t_k) + r_i - r_j\big)\right] \\
& + d_i u_i^{ta}(t_k) + \sum_{j \in N_i} u_{ij}^{a}\big(\|x_{ij}(t_k)\|\big) \\
& + \sum_{j \in N_{io}} u_{ih}^{\beta}\big(\|x_i(t_k) - o_h(t_k)\|\big)
\end{aligned}
\tag{15}
$$

4.1.2. Constructing the Lyapunov Function

Defining

$$
\begin{aligned}
x(t) &\triangleq \text{col}\{x_1(t), x_2(t), \ldots, x_N(t)\} \\
r &\triangleq \text{col}\{r_1, r_2, \ldots, r_N\} \\
\Delta &\triangleq De - A \\
D &\triangleq \text{col}\{0, 0, \ldots, 0, 1\} \\
u^{ta}(t) &\triangleq \text{col}\{u_1^{ta}(t), u_2^{t\alpha}(t), \ldots, u_N^{t\alpha}(t)\} \\
u^{\alpha}(t) &\triangleq \text{col}\{u_1^{\alpha}(t), u_2^{\alpha}(t), \ldots, u_N^{\alpha}(t)\} \\
u^{\beta}(t) &\triangleq \text{col}\{u_1^{\beta}(t), u_2^{\beta}(t), \ldots, u_N^{\beta}(t)\}
\end{aligned}
$$

In addition, set $d(t) = t - t_k, t_k + \tau_k \leq t \leq t_{k+1} + \tau_{k+1}$. We can launch $\tau_k \leq d(t) \leq h + \tau_{k+1}$, then it can be further concluded that $\tau_m \leq d(t) \leq h + \tau_M$. For the convenience of analysis, write $d_m = \tau_m, d_M = h + \tau_M$, that is, $d_m \leq d(t) \leq d_M$. Then the equation of state of AGVs can be simplified as:

$$
\dot{x}(t) = Bx(t) - K\Delta_t[x(t - d(t)) + r] + u^{ta}(t) + u^{\alpha}(t) + u^{\beta}(t)
\tag{16}
$$

where, Δ_t correspond to the Laplacian matrix at time t.

Referring to [10], the Lyapunov function is constructed as follows:

$$
V(t) = V_1(x(t), t) + V_2(x(t), t) + V_3(x(t), t)
\tag{17}
$$

where,

$$
\begin{aligned}
V_1(x(t), t) ={} & x^T(t)Px(t) \\
V_2(x(t), t) ={} & \int_{t-d_m}^{t} e^{s-t}x^T(s)Q_1 x(s)\,ds \\
& + \int_{t-d_M}^{t-d_m} e^{s-t}x^T(s)Q_2 x(s)\,ds \\
V_3(x(t), t) ={} & d_m \int_{-d_m}^{0} \int_{t+\theta}^{t} e^{s-t}\dot{x}^T(s)R_1 x(s)\,ds\,d\theta \\
& + \sigma \int_{-d_M}^{-d_m} \int_{t+\theta}^{t} e^{s-t}x^T(s)R_2 x(s)\,ds\,d\theta
\end{aligned}
$$

where, $P > 0, Q_1 > 0, Q_2 > 0, R_1 > 0, R_2 > 0, d_M > 0, d_m > 0, \sigma = d_M - d_m$. To simplify the representation, denote a block matrix by $H_{ij} = H_i - H_j$. For example: $i = 1, 2, \ldots 5, H_2 = [0, I, 0, 0, 0], H_{14} = [I, 0, 0, -I, 0]$

4.1.3. Calculation of System Stability Conditions

Using the above functions, the following conclusion can be obtained.

Theorem 1. *Set $d_m > 0, d_M > 0, a > 0$, if there exist real matrices $P > 0, Q_1 > 0, Q_2 > 0, R_1 > 0, R_2 > 0$, scalar $b > 0$ and a real matrix S of appropriate dimensions, such that the following inequalities holds, then the system is stable.*

$$\begin{bmatrix} R_2 & S \\ * & R_2 \end{bmatrix} \geq 0, \begin{bmatrix} \phi & \Xi^T \Re \\ * & -\Re \end{bmatrix} < 0 \tag{18}$$

where,

$$\begin{aligned}
\phi =& H_1^T P \Xi + \Xi^T P H_1 + H_1^T (aP + Q_1) H_1 \\
&+ H_3^T \left[e^{-d_m}(Q_2 - Q_1) \right] H_3 - b \left(H_5^T H_5 + H_6^T H_6 + H_7^T H_7 \right) \\
&- H_4^T e^{-d_M} Q_2 H_4 - H_{13}^T e^{-d_m} R_1 H_{13} \\
&- e^{-d_M} \begin{bmatrix} H_{24} \\ H_{32} \end{bmatrix}^T \begin{bmatrix} R_2 & S \\ S & R_2 \end{bmatrix} \begin{bmatrix} H_{24} \\ H_{32} \end{bmatrix} \\
\Xi =& B H_1 - K \Delta_t (H_2 + r) + H_5 + H_6 + H_7 \\
\Re =& d_m^2 R_1 + \sigma^2 R_2
\end{aligned}$$

Proof of Theorem 1. For $t_k + \tau_k \leq t \leq t_{k+1} + \tau_{k+1}$, Set

$$\begin{aligned}
W(t) =& \dot{V}(t) + a V_1(x(t), t) \\
&- b \left[(u^{ta}(t))^T u^{ta}(t) + (u^\alpha(t))^T u^\alpha(t) + (u^\beta(t))^T u^\beta(t) \right]
\end{aligned} \tag{19}$$

We have

$$\begin{aligned}
W(t) \leq& 2x^T(t) P x(t) + x^T(t)(aP + Q_1) x(t) \\
&- b \left[(u^{ta}(t))^T u^{ta}(t) + (u^\alpha(t))^T u^\alpha(t) + (u^\beta(t))^T u^\beta(t) \right] \\
&- e^{-d_m} x^T(t - d_m)(Q_2 - Q_1) x(t - d_m) \\
&+ e^{-d_M} x^T(t - d_M) Q_2 x(t - d_M) + x^T(t) \Re x(t) \\
&- e^{-d_m} \xi_1 - e^{-d_M} \xi_2
\end{aligned} \tag{20}$$

where, $\xi_1 = -d_m \int_{t-d_m}^t \dot{x}^T(s) R_1 \dot{x}(s) ds, \quad \xi_2 = -\sigma \int_{t-d_M}^{t-d_m} \dot{x}^T(s) R_2 \dot{x}(s) ds$.

Define $\psi(t) = \left[x^T(t), x^T(t - d(t)), x^T(t - d_m), x^T(t - d_M), (u^{ta}(t))^T, (u^\alpha(t))^T, (u^\beta(t))^T \right]^T$.

Lemma 1 ([15]). *If there exists a constant matrix $R > 0$ and $R \in \mathbb{R}^{n \times n}$, scalar $\tau > 0$, and vector function $\dot{w} : [-\tau, 0] \to \mathbb{R}^n$ such that the following integral inequality holds:*

$$-\tau \int_{t-\tau}^t \dot{w}^T(s) R \dot{w}(s) ds \leq -[w(t) - w(t - \tau)]^T R [w(t) - w(t - \tau)] \tag{21}$$

Lemma 2 ([16]). *For given positive integers n, m, the scalar η in the interval $(0,1)$, and the given matrix $R > 0$, two matrices W_1 and W_2, define the function $f(\eta, R)$ for all vector $\varphi(t)$ in $\mathbb{R}^m$ as:*

$$f(\eta, R) = \frac{1}{\eta} \varphi^T(t) W_1^T R W_1 \varphi(t) + \frac{1}{1 - \eta} \varphi^T(t) W_2^T R W_2 \varphi(t) \tag{22}$$

If there exists a matrix $S \in \mathbb{R}^{n \times n}$ such that $\begin{bmatrix} R & S \\ S & R \end{bmatrix} \geq 0$, then the following statement holds:

$$\min_{\eta \in (0,1)} f(\eta, R) \geq \varphi^T(t) \begin{bmatrix} W_1 \\ W_2 \end{bmatrix}^T \begin{bmatrix} R & S \\ S & R \end{bmatrix} \begin{bmatrix} W_1 \\ W_2 \end{bmatrix} \varphi(t) \tag{23}$$

From Lemmas 1 and 2, we can get:

$$\xi_1 \leq -\psi^T(t) H_{13}^T R_1 H_{13} \psi(t) \tag{24}$$

Note that

$$
\begin{aligned}
\xi_2 &= -\sigma \int_{t-d_M}^{t-d(t)} x^T(s) R_2 x(s) ds - \sigma \int_{t-d(t)}^{t-d_m} x^T(s) R_2 x(s) ds \\
&\leq -\frac{\sigma}{d_M - d(t)} \psi^T(t) H_{24}^T R_2 H_{24} \psi(t) \quad - \frac{\sigma}{d(t) - d_m} \psi^T(t) H_{32}^T R_2 H_{32} \psi(t) \\
&\leq -\psi^T(t) \begin{bmatrix} H_{24} \\ H_{32} \end{bmatrix}^T \begin{bmatrix} R_2 & S \\ S & R_2 \end{bmatrix} \begin{bmatrix} H_{24} \\ H_{32} \end{bmatrix} \psi(t)
\end{aligned}
\tag{25}
$$

In conclusion, $\dot{V}(t) \leq W(t) \leq \psi^T(t)[\phi + \Xi^T \Re \Xi] \psi(t)$. If $\phi + \Xi^T \Re \Xi < 0, \dot{V}(t) < 0$. Using Schur's complement theorem, we can write $\phi + \Xi^T \Re \Xi < 0$ becomes $\begin{bmatrix} \phi & \Xi^T \Re \\ * & -\Re \end{bmatrix} < 0$. □

4.2. Stability Analysis of Systems Considering Information Interaction between Leaders

In practice, information may be exchanged between clusters to allocate resources and keep track of the status of other tasks. So we also take this situation into account. It is assumed that different clusters interact with each other through their leaders and MEC. The state equations and artificial potential field functions of each cluster are still the same as those in the previous section, which are not repeated here. We also simulate this situation in Section 5.

5. Network Topology Optimization for the Stability of MAS

In this section we try to obtain the optimal topology structure on the premise of ensuring the stability of MAS. The goal is to make the formation as stable as possible, because the second smallest eigenvalue of the Laplacian matrix Δ of the formation topology adjacency matrix is an important index affecting the control stability of the system. $\Delta = De - A$. De is the degree matrix. In order to prevent the collision of agents arbitrarily close to each other in the maximization target, and considering the needs of external obstacle avoidance function in real life, the topology optimization problem is transformed into the following problem by referring to [17]:

$$
\begin{aligned}
\max_{x} \ & \lambda_2(\Delta) \\
\text{s.t. } & \|x_i - x_j\|^2 \geq d_\alpha{}^2 \\
& \|x_i - o_h\|^2 \geq d_\beta{}^2
\end{aligned}
\tag{26}
$$

where $i = 1, 2, \ldots, n-1, j = 2, 3, \ldots, n$, and $i < j$. Assuming that there are H obstacles, then $h = 1, 2, \ldots, H$.

Due to the relative distance between agents and the nonlinear correlation of the Laplacian matrix, the above problem is a nonlinear optimization problem. For the convenience of analysis, the following two lemmas are used to transform the problem.

Lemma 3 ([11]). *Consider an m-dimensional subspace $P \subseteq R^n$ composed of vectors $p_i \in R^n, i = 1, 2, \ldots, m$, denoted as $P = [p_1, p_2, \ldots, p_m] \in R^{n \times m}$, then the matrix M satisfies: For any nonzero vector $x \in P$, we have $x^T M x > 0$, if and only if $P^T M P > 0$.*

Lemma 4 ([11]). *For the Laplace matrix Δ, the second smallest eigenvalue $\lambda_2(\Delta) \geq 0$ is equivalent to $P^T \Delta P \geq 0$, where $P = [p_1, p_2, \ldots, p_{n-1}], p_i \in R^n, i = 1, 2, \ldots, m$ is unit orthogonal vectors, which satisfy:*
(1) $p_i^T 1 = 0, i = 1, 2, \ldots, n-1$ (2) $p_i^T p_j = 0, i \neq j$.

From the above two lemmas, we can see that $x^T \Delta x \geq 0$ can be converted to $P^T \Delta P \geq 0$, where P is a matrix composed of nonzero vectors of $1^\perp$. Therefore, the optimization problem can be transformed into the following problem:

$$\max_x \lambda_2(\Delta)$$
$$s.t. \ \|x_i - x_j\|^2 \geq {d_\alpha}^2$$
$$\|x_i - o_h\|^2 \geq {d_\beta}^2 \tag{27}$$
$$P^T \Delta P \geq 0$$

In order to implement the iteration, each step of the iteration maximizes the second smallest eigenvalue, we discretize the constraint. Set $d_{ij}(t_k) = \|x_i(t_k) - x_j(t_k)\|^2$, where t_k is the k th sampling time, then

$$\dot{d}_{ij}(t_k) = 2[\dot{x}_i(t_k) - \dot{x}_j(t_k)]^T [x_i(t_k) - x_j(t_k)] \tag{28}$$

Let $x(t_k) = x(m), \dot{x}(t_k) = \frac{x(m+1) - x(m)}{t_\Delta}$, where m is the number of iterations, so

$$\frac{d_{ij}(m+1) - d_{ij}(m)}{t_\Delta} = 2\left[\frac{x_i(m+1) - x_i(m)}{t_\Delta} - \frac{x_j(m+1) - x_j(m)}{t_\Delta}\right]^T \times [x_i(m) - x_j(m)] \tag{29}$$

If we simplify the above equation, we can obtain

$$d_{ij}(m+1) - d_{ij}(m)$$
$$= 2[x_i(m+1) - x_i(m) - x_j(m+1) - x_j(m)]^T \times [x_i(m) - x_j(m)]$$
$$= 2[x_i(m+1) - x_j(m+1)]^T [x_i(m) - x_j(m)] - 2[x_i(m) - x_j(m)]^T [x_i(m) - x_j(m)]$$
$$= 2[x_i(m+1) - x_j(m+1)]^T [x_i(m) - x_j(m)] - 2d_{ij}(m)$$

which is equal to

$$d_{ij}(m+1) + d_{ij}(m) = 2[x_i(m+1) - x_j(m+1)]^T [x_i(m) - x_j(m)] \tag{30}$$

Similarly, if we define $d_{ih}(t_k) = \|x_i(t_k) - o_h(t_k)\|^2$, we can obtain

$$d_{ih}(m+1) + d_{ih}(m) = 2[x_i(m+1) - o_h(m+1)]^T [x_i(m) - o_h(m)] \tag{31}$$

Therefore, the non-convex constraint of (27) is transformed into:

$$\max_{x(m+1)} \lambda_2(\Delta)$$
$$s.t. \ d_{ij}(m+1) + d_{ij}(m) = 2[x_i(m+1) - x_j(m+1)]^T \times [x_i(m) - x_j(m)]$$
$$d_{ij}(m+1) > {d_\alpha}^2$$
$$d_{ih}(m+1) + d_{ih}(m) = 2[x_i(m+1) - o_h(m+1)]^T \times [x_i(m) - o_h(m)] \tag{32}$$
$$d_{ih}(m+1) > {d_\beta}^2$$
$$P^T \Delta(m) P \geq 0$$

The above algorithm was iterated until the eigenvalue could not be further increased. In this paper, FMINCON was used to solve (32), and Laplacian matrix is affected by the channel environment.

6. Simulations and Performance Evaluation

In this section, we make simulations to evaluate the performance of the proposed algorithm. Consider a 200 m × 200 m industrial park, in which there are several clusters of AGVs, each cluster has its own transport task, and the AGVs in the cluster use Wi-Fi for information interaction. There is information interaction between some clusters to cooperatively complete the unloading of computing tasks such as real-time path planning, and the clusters are connected through 5G access to edge layer servers. In the simulation, the obstacle is abstracted as a particle randomly distributed in the industrial park. By setting a target point for each cluster, the target point applies attractive force to the leader, and then the leader pushes the whole group of AGVs to move to the target point. If there is an obstacle on the way, repulsive force will be applied between the obstacle and AGVs to avoid collision. In this process, the topological connection of the cluster may be changed.

6.1. Performance Evaluation of AGVs within a Single Cluster

In this section, the working process of AGVs within a single cluster in the industrial park is simulated. The specific parameters are shown in Table 1. We select a cluster in the industrial park, and the simulation environment is a two-dimensional space of 20 m × 20 m.

Table 1. The simulation parameters.

Parameters	Meaning	Value
n	Path loss index	2.5
P_{ij}	Transmit power between agents i and j (dB)	20
G_{ij}^a	Antenna gain between agents i and j (dBi)	16
γ	Minimum signal-to-noise ratio threshold (dB)	2
σ^2	Noise power (W)	0.04
d_M	Upper bound on time delay (s)	0.02
h	AGVs internal sampler sampling interval (s) (dB)	0.01
d_m	Lower bound on time delay (s)	0.005
v_{max}	Maximum velocity of AGVs in the x and y directions (m/s)	0.5
N	Number of AGVs	6
$goal$	Target point	[10, 8]
$obtemp$	Position of obstacle	[5, 2.3; 4, 9]
h	AGVs internal sampler sampling interval (s) (dB)	0.01
$initf_1$	Initial position	[−4, −1.5; −2, −2.5; −3, −2.4; −2.5, −4; −1, −4.5; −0.5, −3]
d_α	Threshold distance between AGVs to trigger obstacle avoidance (m)	1.5
d_β	Threshold distance between AGVs and obstacle to trigger obstacle avoidance (m)	1.5
r	Maximum communication radius between AGVs (m)	5.5
d_{fl}	Ideal relative position of AGVs and Leader	[−1.5, 1.5; 1.5, 1.5; −3, 0; −1.5, −1.5; 1.5, −1.5; 0, 0]

It can be seen from Section 4 that certain conditions must be met to ensure the stability of the system. Therefore, we use LMI to solve the value of each parameter under the condition of ensuring stability. In the environment set in this paper, the topology changes randomly with the environment, and the change of parameters is relatively complex.

For simple calculation, each agent in this paper adopts the same controller gain at the same time, but the controller gain will change at different times, that is, under different topologies. Therefore, the controller gain changes several times in the whole process. For the sake of simplicity, the generated controller gain is no longer enumerated in this paper, and only a simulation diagram comparison is given. In this process, the preset communication connection threshold is 0.6, that is $a_{ij}(t) = 1$ when $p_\gamma^{ij}(\Gamma_{ij}(t) > \gamma) \geq 0.6$, there is information interaction between the two AGVs.

Figure 4 shows four stages of a single cluster in completing a task. The black circle represents the following AGV, the green circle represents the leader, the blue pentagram represents the target point of each cluster, and the Red Cross represents the obstacle. For ease of observation, we sample every 0.1 s and record the position of the AGVs. The sampling point is denoted as k. In this paper, $k = 1, k = 85, k = 270$ and $k = 500$ are respectively selected and presented in Figure 4 as examples of the four situations. As can be seen from the figure, in the initial case, AGVs are closely connected. According to the ideal minimum distance between AGVs set in Table 1, firstly, AGVs in the cluster need to keep a certain distance from each other to prevent collision during driving. The position state of AGVs after internal adjustment is shown in Figure 4 (II). Later, some AGVs encounter obstacles and conduct external obstacle avoidance, which will lead to changes in the distance between AGVs and the connection topology. When the leader continues to move after the external obstacle avoidance is completed and reaches the target point, the topology is shown in Figure 4 (IV), which conforms to the preset desired formation.
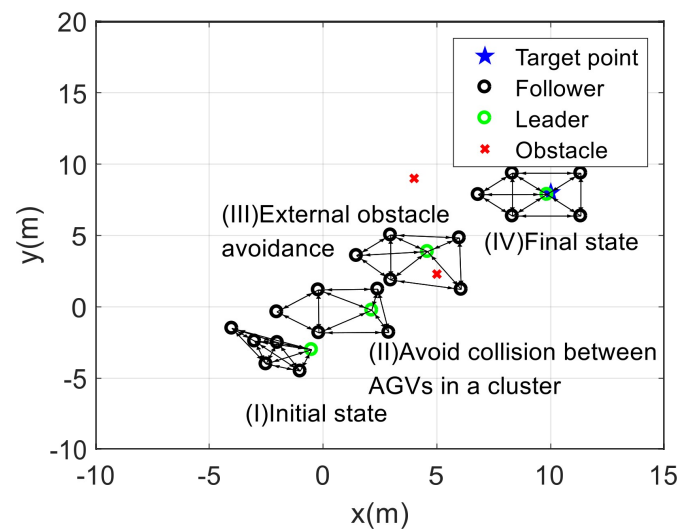
Figure 4. Movement process of a single cluster. The figure shows the formation in four cases. The four cases are: initial state, avoid collision between AGVs in a cluster, External obstacles avoidance, final state.

As can be seen from the above process, the whole system remains stable in the case of external environmental interference in the movement process. We can see the effectiveness of the artificial potential field algorithm for obstacle avoidance in the whole system through the position trajectory of the whole process. As shown in Figure 5, each AGV in the cluster is close to each other at the initial time, so internal obstacle avoidance is carried out to avoid possible collisions. When follower 2, follower 5 and the leader are close to the external obstacles, they have an obvious curve of obstacle avoidance and carry out external obstacle avoidance. These two points show that the algorithm adopted in this paper is effective.
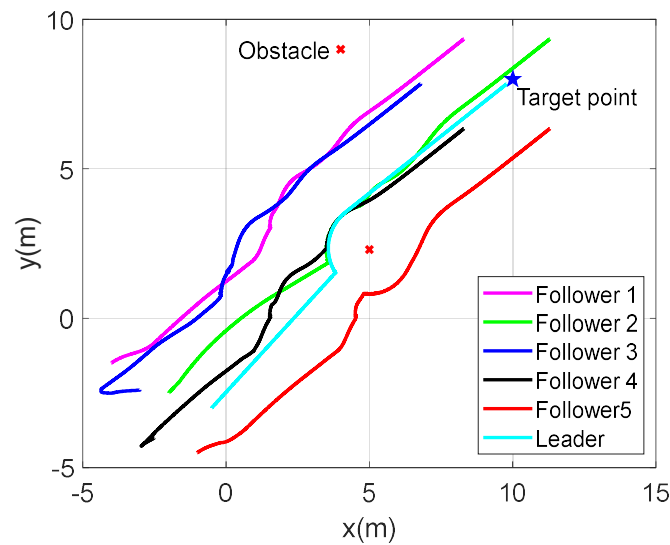
Figure 5. Motion trajectories of AGVs in a single cluster. The figure shows the trajectories of the tasks performed by each AGV.

Next we change the channel parameters to observe the change in topology and motion trajectory. Since the antenna gain is too low, the connection between AGVs may be disconnected due to the increase of distance during external obstacle avoidance, we increase the antenna gain of the AGVs to 17.2 dBi, and still select the sampling points $k = 1, k = 85, k = 270$, and $k = 500$. Figure 6 shows the whole process. The topology changes a little bit during the motion.
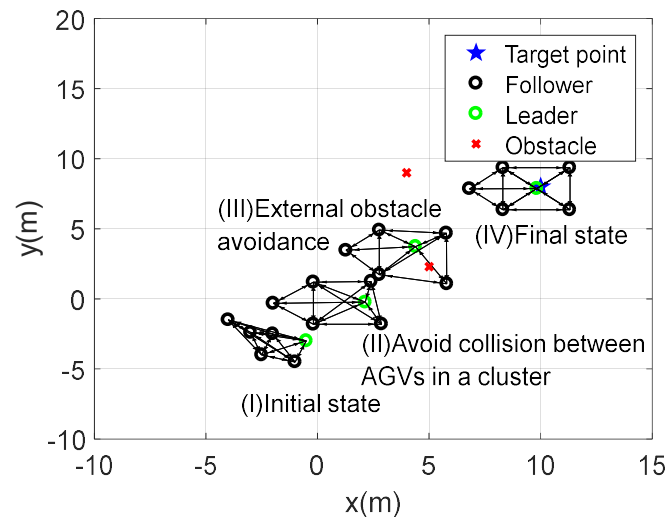
Figure 6. Single cluster motion process after modifying channel environment. The figure shows the formation in four cases. The four cases are: initial state, avoid collision between AGVs in a cluster, External obstacles avoidance, final state.

It can be seen that the change of channel environment will affect the change of topology structure, and the change of topology structure will affect the stability of the whole system. In order to compare the stability under different channel conditions, the aggregation coefficient related to the cluster center distance of AGV is introduced in this paper. The aggregation coefficient is defined as $C = \frac{1}{N}\|x - 1_N \otimes \bar{x}\|$, where $x = \left(x_1^T, \ldots, x_N^T\right)^T$, $\bar{x} = \frac{1}{N}\sum_{i=1}^{N} x_i(t)$. The larger the aggregation coefficient C is, the lower the aggregation degree of MAS is and the more dispersed the AGV distribution is. The smaller C is, the higher degree of MAS aggregation and the more concentrated AGV distribution. Figure 7

compares the aggregation coefficient curves of the AGVs under two different channel environments, reflecting the influence of the channel environment on MAS stability. If the aggregation coefficient curve does not rise indefinitely, that is, when it is always less than a certain constant, it indicates that no AGV in MAS has left the team, and it keeps convergence and good stability in the whole process of completing the task.
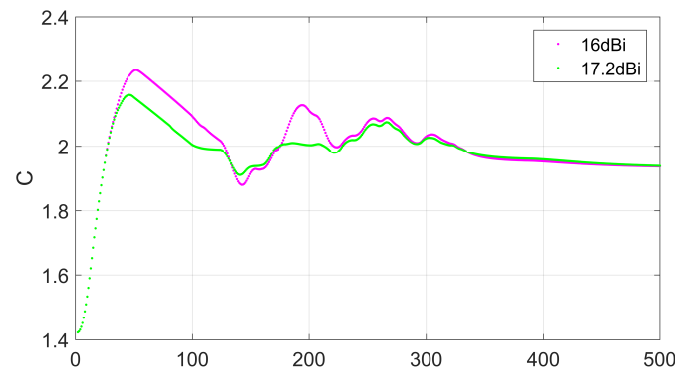
Figure 7. Aggregation coefficient of AGVs with antenna gain of 16 dBi and 17.2 dBi. Different antennas are used to represent different channel conditions. The figure shows the aggregation coefficients at each sampling point under different channel conditions.

As can be seen from Figure 7, at the initial position, the distance between the agents should not be too large according to the ideal relative distance and artificial potential field force. After the antenna gain is improved, MAS can be aggregated faster. When encountering obstacles, it is necessary to stay away from the obstacles and keep a distance between the AGVs, so the aggregation coefficient will fluctuate from big to small. After the obstacle avoidance is completed, it will be adjusted to the desired formation, and the convergence degree will be consistent.

This section mainly verifies the feasibility of the governing equations set in Section 4, that is, the MAS can complete the obstacle avoidance and transportation tasks on the premise of ensuring stability, and directly reflects the influence of the channel environment on the topology and system stability through the simulation diagram.

6.2. Performance Evaluation of AGVs in Inter-Clusters

In this section, the workshop working process in the industrial park is simulated when the information interaction of multiple clusters is considered. To facilitate the experiment, we only select the case of two clusters.

To observe the movement of the two clusters, we selected a two-dimensional space with a simulation environment of 30 m × 40 m to verify the stability of the formation system composed of AGVs of the two clusters and the feasibility of formation transformation according to the channel environment. The channel environment is the same as that in the single cluster case in the previous section, and only the changed parameters are listed here. The left base station is labeled as base station 1, the right base station is labeled as base station 2. The left cluster is labeled as cluster 1, and the right cluster is labeled as cluster 2. The position information of obstacles changes as $[5, 4; 4, 8; 6, 5; 26, 10; 23, 15]$. The target point of cluster 1 is changed to $[10, 10]$. The target point of cluster 2 is set as $[30, 13]$. The initial position of cluster 1 is the same as that in the previous section. The initial position of cluster 2 is $[12, 6.5; 13.5, 8.5; 13.5, 6.5; 14, 11.5]$, and the ideal position of each AGV in cluster 2 relative to the leader is $[-1.5, 1.5; 1.5, 1.5; -1.5, -1.5; 0, 0]$. Figure 8 shows the motion of the two clusters. The black diamond represents the base station of the edge layer. Consider the two base stations located at $[-85, 100]$ and $[105, 100]$. In order to make the simulation diagram clear, the two base stations are respectively placed at $[5, 25]$ and $[25, 25]$ when the simulation diagram is generated, and they are still set at $[-85, 100]$ and $[105, 100]$ in the simulation code.
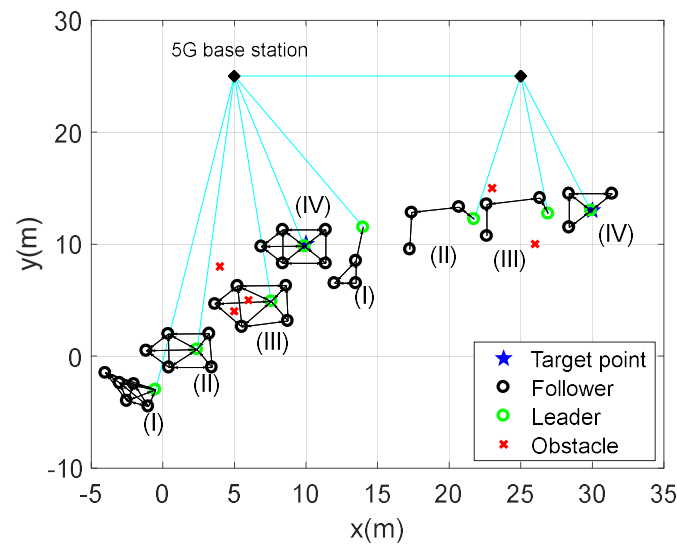
Figure 8. Motion process when information interaction between clusters is considered. The figure describes the motion of clusters in the process of performing the task, which can be also divided into four cases. In the process of movement, cluster heads will select the base station with better channel conditions to connect, and other clusters will be connected through the base station. The blue lines in the figure represent 5G connections.

Using the formula $Ca_{ik} = W_k \log_2 \left(1 + \frac{P_i G_i^a d_{ik}^{-n}}{n_0 W_k} \right)$ proposed by Section 3.1 to calculate the channel capacity. The base station set at $[-85, 100]$ has a bandwidth of 10.2 MHz, and the bandwidth of the base station located at $[105, 100]$ is 10 MHz. The noise power spectral density is -174 dbm, and the antenna gain of AGVs and the transmit power of the AGVs are the same as those in Section 6. Each leader selects the channel with a larger channel capacity for data transmission. At the initial point, $Ca_{11} = 192.45$ Mb/s, $Ca_{12} = 185.31$ Mb/s, $Ca_{21} = 192.57$ Mb/s, $Ca_{22} = 190.71$ Mb/s. It can be seen that both clusters are connected with the base station 1, as shown in (I) in Figure 8. It can be seen from the figure that with the constant movement of the AGVs, the connection between the leader and the base station will change. In the figure, (I), (II), (III) and (IV) respectively represent the initial state of the cluster, the control of intra-cluster collision avoidance by the AGVs, external obstacle avoidance and the final state.

It can also be seen from the above process that the whole system remains stable during the movement. Based on the previous section, this section intuitively shows the specific information interaction between clusters and how to choose the topology structure of interaction. The movement of each cluster will affect the connection between the leader and the base station. During the movement, it will judge which base station can be connected to obtain the maximum uplink rate.

6.3. Performances of Network Topology Optimization

Because the main difference between a single cluster and multiple clusters for information interaction is reflected in how to connect and exchange information through the base station, the latter includes the former. Therefore, we directly use the multi-cluster model to optimize the topology within the cluster first, then deduce the channel conditions that meet the requirements according to the optimized topology within the cluster, and finally explore how the connection with the base station changes according to the new channel conditions.

Topology construction is carried out according to the optimization proposed in Section 5, considering the information interaction between clusters. Figure 9 selects two sampling points $k = 200$ and $k = 434$ with different optimized topologies. In the process of completing the transportation task, in order to avoid obstacles, one formation cannot

be maintained all the time, and the optimal formation will change when the external environment changes. From the reconstructed formation, it can be seen that the AGVs in the formation are clustered as much as possible under the constraints of internal and external distance from obstacles to improve the second smallest eigenvalue of the Laplacian matrix.
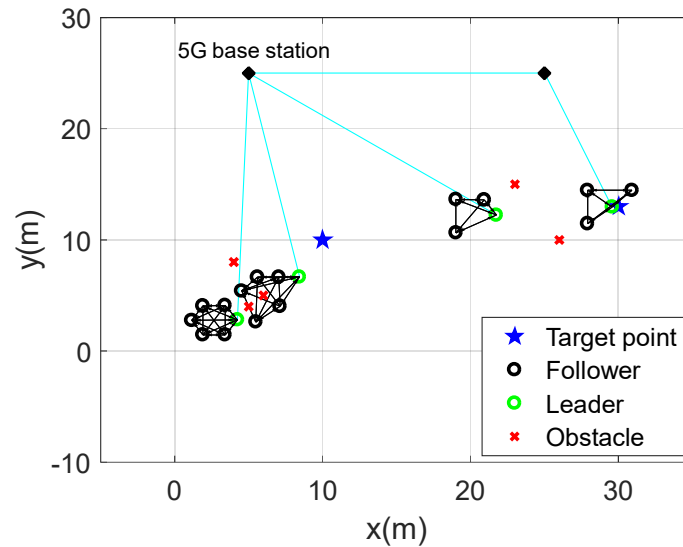
Figure 9. Optimal topology considering information interaction between two clusters. The figure shows the formation of the two sampling points in the task execution process of the two clusters after optimization. At the first sampling point, cluster 1 remains in the desired shape, while cluster 2 is being adjusted. At the second sampling point, cluster 1 is avoiding obstacles and cluster 2 is completing its task and maintaining the desired formation.

In Figure 9, we can observe that the second smallest eigenvalues of the Laplacian matrix of the two clusters optimized without interference from external obstacles are 6 and 4, respectively.

We select the cluster with a more complex structure on the left to compare the stability of the system before and after optimization. The aggregation coefficient before and after topology optimization is shown in Figure 10, and the speed before obstacle avoidance is shown in Figure 11. After optimization, the aggregation coefficient is significantly reduced, the position of the AGVs is relatively compact, The speed convergence is faster, and the stability is improved, which indicates the effectiveness of the optimization method.
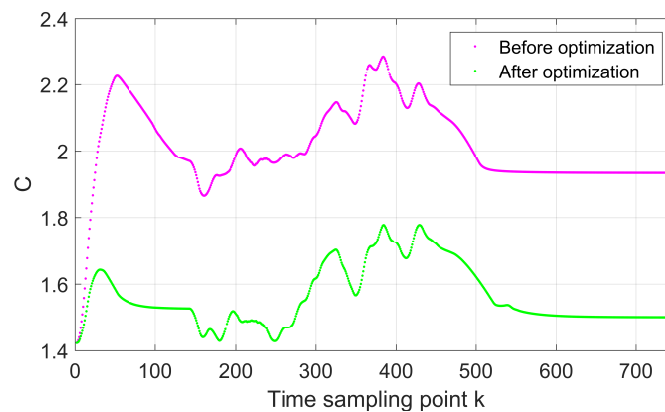
Figure 10. Aggregation coefficient of cluster 1 before and after optimization. The magenta dots and green dots respectively represent the clustering coefficients at each sampling point before and after optimization.
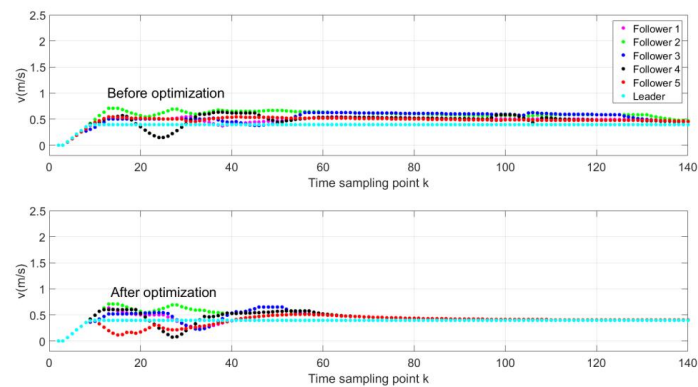
Figure 11. Velocity of cluster 1 before and after optimization. The figure above represents the speed changes of each AGV before optimization, while the figure below represents the speed changes of each AGV after optimization.

In this section, we focus on the optimized topology of the device layer, and then we continue to discuss the overall topology connection including the edge layer.

To complete the simulation process according to the optimal topology shown in the previous section, it is necessary to improve the conditions under which information interaction can take place. Based on the set simulation parameters, due to the information interaction between the two clusters, the AGV antenna gain of cluster 1 can be increased to 18.9 dBi, and the AGV antenna gain of cluster 2 can be increased to 19.2 dBi, which means the optimal topology connection can be realized. At this time, the channel environment has also changed, and the connection between the leader and the base station has also changed. To facilitate comparison, the connection between the cluster and the base station before the optimization is placed below in the simulation. If the leader is connected to base station 1 , the value is -1, and if it is connected to base station 2 , it is -2. The connection between the optimized cluster and the base station is placed on the top. If the leader is connected to base station 1, the value is 1 , and if it is connected to base station 2, it is 2 .

Figure 12 shows that cluster 1 is always connected to base station 1 before and after optimization, and cluster 2 will change its connection to the base station with movement. Before topology optimization, base station switching occurs in cluster 2 when the sampling point sequence $k = 78$. After optimization, base station switching occurs in cluster 2 at $k = 90$. Therefore, when we set the channel environment for the optimized intra-cluster topology, the topological connections between clusters will also change. The integrated and optimized intra-cluster topology and the changed inter-cluster topology are the optimized topologies considering inter-cluster. information interaction. Thus, we obtain the overall optimal topology including the device layer and the edge layer.
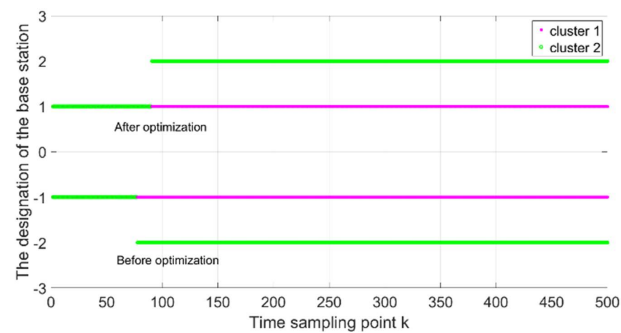
Figure 12. Connection condition between cluster and base station before and after optimization of topology structure. 1 and −1 of the ordinate represent the connection between base station 1 after and before optimization respectively. 2 and −2 of the ordinate represent the connection between each cluster and base station 2 after and before optimization respectively.

7. Conclusions

In this paper, we study the stability of time-varying topology considering delay and obstacle avoidance and the optimization method of network topology in the industrial park scenario. Conditions to ensure the stability of the system are obtained, and the influence of the channel environment on the system performance is verified. In addition, the performance of the system under the topology before and after optimization is compared by with the simulation to verify the effectiveness of the optimization method. Finally, according to the optimized topology, the channel environment that meets the needs of this topology is deduced. Indeed, the simulation results show that the proposed model and algorithm are effective. Now we only consider the delay generated in the transmission process and ignore the computation and processing delay. In addition, we did not consider clock synchronization. Therefore, a possible direction for future research is MAS stability analysis considering clock synchronization and more delay. In addition, using artificial intelligence method for path planning is another possible direction for future research.

Author Contributions: Conceptualization, J.F.; methodology, J.F.; software, J.F.; validation, J.F.; writing—original draft preparation, J.F.; visualization, J.F.; writing—review and editing, L.Z., X.Z. and Y.W.; project administration, L.Z. and X.Z.; funding acquisition, X.Z. All authors have read and agreed to the published version of the manuscript.

Data Availability Statement: No additional data are available.

References

1. Liu, H.; Fang, H.; Mao, Y.; Cao, H.; Jia, R. Distributed flocking control and obstacle avoidance for multi-agent systems. In Proceedings of the 29th Chinese Control Conference, Beijing, China, 29–31 July 2010; pp. 4536–4541.
2. Yin, Y.; Shi, Y.; Liu, F.; Teo, K.L.; Wang, S. Second-Order Consensus for Heterogeneous MASs with Input Constraints. *Neurocomputing* **2019**, *351*, 43–50. [CrossRef]
3. Xie, D.; Chen, J. Consensus problem of data-sampled networked multi-agent systems with time-varying communication delays. *Trans. Inst. Meas. Control.* **2013**, *35*, 753–763. [CrossRef]
4. Wang, C.; Zuo, Z.; Sun, J.; Yang, J.; Ding, Z. Consensus disturbance rejection for Lipschitz nonlinear multi-agent systems with input delay: ADOBC approach. *J. Frankl. Inst.* **2017**, *354*, 298–315. [CrossRef]
5. Iqdal, M.; Kolios, X.; Polycarpou, M. Finite- and Fixed-Time Consensus Protocols for Multi-Agent Systems with Time-Varying Topologies. *IEEE Control. Syst. Lett.* **2022**, *6*, 1568–1579.
6. Gong, Y.; Wen, G.; Peng, Z.; Huang, T.; Chen, Y. Observer-Based Time-Varying Formation Control of Fractional-Order Multi-Agent Systems with General Linear Dynamics. *IEEE Trans. Circ. Syst. Express Briefs* **2020**, *67*, 82–86. [CrossRef]

7. Ge, S.S.; Liu, X.; Goh, C.-H.; Xu, L. Formation Tracking Control of Multi-agents in Constrained Space. *IEEE Trans. Control. Syst. Technol.* **2019**, *24*, 992–1003. [CrossRef]

8. Zhao, P. Design of UAV Formation and Obstacle Avoidance Control System Based on Virtual Navigator. Master's Dissertation, University of Electronic Science and Technology of China, Chengdu, China, 2021.

9. Yun, W.J.; Park, S.; Kim, J.; Shin, M.; Jung, S.; Mohaisen, D.A.; Kim, J.H. Cooperative Multiagent Deep Reinforcement Learning for Reliable Surveillance via Autonomous Multi-UAV Control. *IEEE Trans. Ind. Inform.* **2022**, *18*, 7086–7096. [CrossRef]

10. Ding, L.; Zheng, W. Network-Based Practical Consensus of Heterogeneous Nonlinear Multi-agent Systems. *IEEE Trans. Cybern.* **2017**, *47*, 1841–1851. [CrossRef] [PubMed]

11. Hao, L. UAV formation Algorithm under Multi-Path Channel Based on Communication Topology Optimization. Master's Dissertation, Harbin Institute of Technology, Harbin, China, 2019.

12. Sarafraz, M.S.; Tavazoei, M.S. A Unified Optimization-Based Framework to Adjust Consensus Convergence Rate and Optimize the Network Topology in Uncertain Multi-Agent Systems. *IEEE/CAA J. Autom. Sin.* **2021**, *8*, 1539–1548. [CrossRef]

13. Shannon, C.A. *Claude E. Shannon: Collected Papers*; Wiley-IEEE Press: Hoboken, NJ, USA, 1993.

14. Reynolds, C. Flocks, Herds and Schools: A Distributed Behavioral Model. *Comput. Graph.* **1987**, *21*, 25–34. [CrossRef]

15. Han, Q. Absolute stability of time-delay systems with sectorbounded nonlinearity. *Automatica* **2005**, *41*, 2171–2176. [CrossRef]

16. Park, P.; Ko, J.W.; Jeong, C. Reciprocally convex approach to stability of systems with time-varying delays. *Automatica* **2011**, *47*, 235–238. [CrossRef]

17. Kim, Y.; Mesbahi, M. On maximizing the second smallest eigenvalue of a state-dependent graph Laplacian. *IEEE Trans. Autom. Control.* **2006**, *51*, 116–120. [CrossRef]